Thrombin Activity Is Unaltered by N-Terminal Truncation of Factor XIII Activation Peptides†

Giulia Isetti and Muriel C. Maurer*

Department of Chemistry, University of Louisville, 2320 South Brook Street, Louisville, Kentucky 40292

Received January 28, 2004

ABSTRACT: In blood coagulation, thrombin helps to activate factor XIII by cleaving the activation peptide at the R37−G38 peptide bond. The residues N-terminal to the scissile bond are important in determining rates of hydrolysis. Solution studies of wild-type and mutant peptides of factor XIII AP (28−37) suggest residues P_4−P_1 are most critical in substrate recognition. By contrast, the X-ray crystal structure of FXIII AP (28−37) displays all of the residues, P_{10}−P_1, interacting with the thrombin active site in a conformation similar to that of fibrinogen Aα (7−16) [Sadasivan, C., and Yee, V. C. (2000) *J. Biol. Chem. 275*, 36942−36948]. Peptides were therefore synthesized with the N-terminal P_{10}−P_6 residues removed to further characterize interactions of thrombin with factor XIII activation peptides. The truncations have no adverse effects on thrombin's ability to bind and to hydrolyze the shortened peptides. The wild-type FXIII AP (33−41) V34 sequence actually exhibits a decrease in K_m relative to the longer (28−41) sequence whereas the cardioprotective FXIII AP (33−41) V34L exhibits a further increase in k_{cat} relative to its longer parent sequence. One-dimensional proton line broadening NMR and 2D transferred-NOESY studies indicate that the shortened peptides maintain similar bound conformations as their FXIII AP (28−37) counterparts. Furthermore, the distinctive NOE between the L34 and P36 side chains is preserved. Kinetic and NMR studies thus reveal that the N-terminal portions of FXIII AP (28−37) (V34 and V34L) are not necessary for effective interaction with the thrombin active site surface. FXIII activation peptides bind to thrombin in a manner more like PAR1 than fibrinogen Aα.

In blood coagulation, the serine protease thrombin (*1*−*3*) cleaves specific Arg−Gly bonds within the N-terminal portion of the Aα and Bβ chains of fibrinogen $(A\alpha B\beta\gamma)_2$, thereby releasing fibrinopeptides A and B. Removal of these peptides leads to exposure of fibrin polymerization sites that react to form an insoluble clot (*2*, *4*). Thrombin also helps to activate the transglutaminase factor XIII (FXIII)[1] by cleaving the Arg37−Gly38 peptide bond (*5*). This hydrolysis permits release of the FXIII activation peptide (FXIII AP) and eventual exposure of the catalytic site. The activated FXIII later catalyzes the formation of γ-glutamyl-ϵ-lysyl covalent cross-links in the fibrin network and in fibrin−enzyme complexes. Thrombin activation of FXIII is significantly enhanced in the presence of fibrin I (*6*−*8*). Fibrin I is proposed to bind to thrombin anion exosite I and assist in promoting interactions between the thrombin active site and the FXIII activation peptide segment. Studies have begun to map the exact sites of contact between thrombin and FXIII (*9*).

In human factor XIII, V34L is a common polymorphism that has been associated with cardioprotective effects. Thrombin activates FXIII V34L more readily than the wild-type FXIII V34 (*10*−*13*). Furthermore, fibrin cross-linked by FXIII V34L can have a finer structure with thinner fibers and smaller pores than fibrin cross-linked by FXIII V34 (*12*, *13*). The protective effects of FXIII V34L occur predominately under high fibrin(ogen) conditions and have been correlated with the formation of a more permeable fibrin structure (*14*). Thrombin cleavage of FXIII V34L results in improvements in both K_m and k_{cat} over the wild-type V34 (*10*−*12*). These effects are seen both in vivo and in vitro (*14*). Similar trends are observed with synthetic peptide models of the FXIII activation peptide segment (*15*).

In addition to hydrolyzing peptides from blood coagulation proteins, thrombin also cleaves protease-activated receptors (PARs). Two key members of this family include PAR1 and PAR4. PAR1 is hydrolyzed by thrombin at the R41−G42 peptide bond and PAR4 at the R47−G48 peptide bond. New N-termini are created that serve as tethered ligands to help to activate these receptors (*16*−*20*).

A review of thrombin substrates indicates that the amino acids N-terminal to the scissile bond make significant contributions to binding and to rates of hydrolysis. Studies using small peptide models conclude that the optimal sequence for the P_3 through P_1 subsites[2] is F/VPR (*21*, *22*). Furthermore, thrombin substrates benefit from having hydrophobic residues at the P_4 and P_2 positions that can promote interactions with the enzyme active site region. A proline is

† Funding for this project is supported by NIH Grant R01 HL68440.

* To whom correspondence should be addressed. Tel: 502-852-7008. Fax: 502-852-8149. E-mail: muriel.maurer@louisville.edu.

[1] Abbreviations: FXIII, blood clotting factor XIII; AP, activation peptide; Fbg Aα, peptide segment from the fibrinogen Aα chain; PAR1, protease-activated receptor 1; PAR4, protease-activated receptor 4; RP-HPLC, reversed-phase high-performance liquid chromatography; MALDI-TOF, matrix-assisted laser desorption ionization time of flight; K_m, Michaelis−Menten kinetic constant; k_{cat}, catalytic constant or turnover number; NMR, nuclear magnetic resonance; TOCSY, total correlation spectroscopy; NOESY, nuclear Overhauser effect spectroscopy.

10.1021/bi049796v CCC: $27.50
Published on Web 03/20/2004

Table 1: Sequences of Thrombin Substrates[a]

	P_9.....P_4.....P_1...
Factor XIII AP **V34** segment	^{28}TVELQG**V**V**PR**GVNL^{41}
Factor XIII AP **V34L** segment	^{28}TVELQG**L**V**PR**GVNL^{41}
Factor XIII AP truncated **V34**	^{33}G**V**V**PR**GVNL^{41}
Factor XIII AP truncated **V34L**	^{33}G**L**V**PR**GVNL^{41}
Fibrinogen Aα chain segment	^{7}D**F**LAEGGG**VR**GPRV^{20}
Thrombin Receptor PAR1 segment	^{32}KATNAT**L**D**PR**SFLL^{45}

[a] These human sequences were taken from the following sources: factor XIII (*24*), fibrinogen Aα chain (*25*), and thrombin receptor PAR1 (*26*).

highly desirable at the P_2 position, and a hydrophobic residue is preferred at the P_3 position (*23*). In addition to its nonpolar character, the proline ensures backbone rigidity for the P_3-P_2 bond that aids in effective binding to the thrombin active site (*23*).

Table 1 shows a series of peptide sequences based on natural thrombin substrates. Factor XIII AP V34, FXIII AP V34L, and PAR1 each have a proline at the P_2 position. Fibrinogen Aα (Fbg Aα), by contrast, has a valine at this position. FXIII AP V34 contains a valine at the P_4 position whereas FXIII AP V34L and PAR1 both contain a leucine at this position. Kinetic and NMR studies have demonstrated that the extra methylene group of FXIII Leu34 allows this P_4 residue to be closer to the P_2 residue Pro36 in the enzyme-bound state (*27*). As a result, the two amino acids can associate more effectively with the thrombin apolar site. This beneficial P_4 to P_2 interaction likely leads to the increased rate of activation of FXIII L34 compared to FXIII V34. NMR and X-ray structures of the PAR1−thrombin complex reveal the same key interactions between the P_4 residue Leu and the P_2 residue Pro (*28*, *29*). PAR1 peptides that target the thrombin active site, however, are not as good substrates as those of the FXIII AP segments (*15*, *18*, *27*). Interactions with thrombin anion exosite I are needed to overcome the difficulties associated with having an acidic residue at the P_3 position (^{38}LDPR^{41}) (*30*).

Peptides based on the fibrinogen Aα sequence can also effectively target the thrombin active site; however, amino acid positions that differ from those of FXIII and PAR1 are employed. Fbg Aα contains within its P_4-P_1 sequence (^{13}GGVR^{16}) a Val at the P_2 position and a Gly at the P_4 position. This sequence lacks an amino acid with a hydrophobic side chain at the P_4 position and also lacks the five-membered proline ring at the P_2 position. Furthermore, the sequence does not exhibit the desirable rigidity about the P_3-P_2 bond. To compensate for this nonoptimal sequence, the distant Phe at the P_9 position and the Leu at the P_8 position are brought back through a unique β-turn conformation to occupy the S_4 specificity pocket on thrombin. This structural feature has been observed by both X-ray and NMR methods (*31*−*36*).

X-ray crystallographic studies on the complex of wild-type factor XIII AP (*28*−*37*) with thrombin have generated interesting results (*37*). The N-terminus assumes a conformation much like that of Fbg Aα (7−16) whereas the C-terminus contains a proline that promotes a conformation similar to that of PAR1. By contrast, 2D transferred-NOESY data suggest that the N-terminus of the bound FXIII AP (28−37) makes little, if any, contact with the enzyme surface in solution and that the P_4-P_1 positions of FXIII AP (28−37) dominate the thrombin-bound structure (*27*).

To address the differences observed between the X-ray crystal structures and the solution NMR studies, the N-termini of the FXIII AP-like sequences were truncated and interactions with thrombin were examined. Peptides based on amino acids 33−41 actually experience improvements in their kinetic properties relative to the longer (28−41) segments. FXIII AP (33−37) V34 exhibits a decrease in K_m versus FXIII AP (28−41) V34, and FXIII AP (33−41) V34L exhibits an enhancement in k_{cat} versus its longer parent sequence. One-dimensional proton line broadening NMR and 2D transferred-NOESY studies indicate that the shortened peptides maintain a similar bound conformation as the FXIII AP (28−37) peptides. Kinetic and NMR studies thus reveal that the N-terminal portions of FXIII AP (28−32) V34 and V34L are not necessary for effective interaction with the thrombin active site surface.

EXPERIMENTAL PROCEDURES

Synthetic Peptides. Peptides based on residues 28−41 of the human FXIII activation peptide were synthesized by SynPep (Dublin, CA). Peptides based on residues 33−41 of the human FXIII AP were synthesized by Giulia Isetti (University of Louisville, Louisville, KY). The amino acid sequences of the peptides are as follows: FXIII AP (28−41), Ac-TVELQGVVPRGVNL-amide; FXIII AP (28−41) V34L, Ac-TVELQGLVPRGVNL-amide; FXIII AP (33−41), Ac-GVVPRGVNL-amide; and FXIII AP (33−41) V34L, Ac-GLVPRGVNL-amide. The purity of the peptides was evaluated by analytical reversed-phase HPLC. Matrix-assisted laser desorption time-of-flight (MALDI-TOF) measurements on an Applied Biosystems Voyager DE-Pro mass spectrometer were used to verify the peptide *m*/*z* values. The concentrations of the peptides in solution were determined by quantitative amino acid analysis (Molecular Analysis Facility, University of Iowa, Iowa City, IA).

Thrombin Preparation. Plasma bovine citrate eluate (Sigma) was dissolved in activation buffer (50 mM Tris, 150 mM NaCl, 0.1% PEG, pH 7.4). The solution was desalted on an Amersham Pharmacia Biotech PD-10 column equilibrated with activation buffer. The thrombin solution was activated by addition of $CaCl_2$ and snake venom (*Echis carinatus*), incubated at 37 °C, and monitored for fibrinogen clotting capability. The BCE/Ca/venom mixture was desalted on a Sephadex G-25 column equilibrated with desalting column buffer (25 mM H_3PO_4, 100 mM NaCl, pH 6.5). The activated thrombin was purified on an Amersham Pharmacia Biotech Mono S cation-exchange column (HR10/10) using a linear gradient of 0−1 M NaCl in 25 mM H_3PO_4, pH 6.5. The pooled thrombin solution was concentrated by ultrafiltration

[2] The P nomenclature system (..., P_3, P_2, P_1, P_1', P_2', P_3', ...) is used to assign the individual amino acid positions on the substrate peptides. The P_1-P_1' peptide bond becomes hydrolyzed by the enzyme. The peptide amino acids to the left of the cleavage site are labeled P_2, P_3, P_4, etc. whereas as those to the right of the cleavage site are labeled P_2', P_3', P_4', etc.

with an Amicon 8010 ultrafiltration cell and a Diaflo YM10 ultrafiltration membrane and then aliquoted and frozen at −70 °C for future use. The final concentration of thrombin was determined using the extinction coefficient $E^{1\%} = 19.5$ at 280 nm (*38*).

For this project, bovine thrombin was used as the enzyme, and the synthetic substrate peptides were based on human sequences. Thrombin exhibits a high degree of sequence conservation between the bovine and human forms (*39*). There are no differences in the residues involving the active site, the thrombin β-insertion loop (also called the Trp^{60D} loop), or the allosteric Na^+ binding site. The minor differences that do exist are not anticipated to interfere with the interaction of the substrate peptides at the thrombin active site surface (*40*).

Kinetics Procedure. The HPLC-based kinetic assay methods were described previously by Trumbo and Maurer (*15*). Briefly, a solution of peptide and assay buffer (50 mM H_3PO_4, 100 mM NaCl, 0.1% PEG, pH 7.4) was heated to 25 °C in a heat block. Hydrolysis was started by the addition of bovine thrombin. The thrombin concentration for the hydrolysis reactions was 2.2 nM for the V34L peptides and 33.6 nM for the V34 peptides. The peptide concentrations for FXIII AP (28−41) and FXIII AP (33−41) were 100−1500 μM whereas the peptide concentrations for FXIII AP (28−41) V34L and FXIII AP (33−41) V34L were 100−1250 μM. At regular intervals, an aliquot of the reaction mixture was removed and quenched in 12.5% H_3PO_4. Peptide peaks were separated by RP-HPLC using a Brownlee Aquapore octyl RP-300 C8 cartridge column on a Waters HPLC system. Thrombin concentration and kinetic time points were chosen such that less than 15% of the total peptide concentration was hydrolyzed within 30 min.

Initial velocities (in micromolar per second) for the thrombin-catalyzed reactions were determined for each peptide concentration from the slopes of product concentrations versus time plots. The results reported represent averages for at least three independent experiments. Kinetic values reported were calculated using nonlinear regression analysis fit to the equation:

$$V = V_{max}/(1 + K_m/[S])$$

using the Marquardt−Levenberg algorithm in Sigma Plot (Jandel Scientific). K_m, V_{max}, and k_{cat} were calculated from the coefficients of this equation.

One-Dimensional Proton Line Broadening and Two-Dimensional Transferred-NOESY NMR. These NMR methods were used to probe the structural features adopted by each FXIII activation peptide-like substrate when bound to thrombin. When free in solution, peptides of less than 15 amino acids in length tumble rapidly and, generally, have little secondary structure. $\omega\tau_c$ approaches 1, giving a sharp 1D proton spectrum and a transferred-NOESY spectrum with few NOEs. When bound to the surface of an enzyme, the same peptide can gain secondary structural features. A macromolecular complex with an increased $\omega\tau_c$ is created and promotes the appearance of large negative NOEs that describe the bound state of the peptide. In a complex, where the peptide is in molar excess of the enzyme and the k_{off} for the peptide is fast, information about this bound state is carried with the peptide as it rejoins the free population. NOEs that describe this bound state dominate the NOESY spectrum (*41*, *42*).

Interactions between the peptide and the enzyme may also be monitored by 1D proton line broadening studies. Peptide protons that come into contact with the larger and more slowly rotating enzyme surface experience changes in T_2 that contribute to line broadening. In the presence of the new chemical environment, changes in proton chemical shift are also possible. Together, these different effects lead to changes in line width and/or line shape that reflects the contributions of the bound conformation transferred to the free population (*41*, *42*).

NMR Sample Preparation and Analysis. An approximately 1:10 ratio of enzyme to peptide was maintained for each complex studied. Sample preparation and analysis procedures similar to those of Trumbo and Maurer (*27*) were employed. Select features are summarized here. The peptides were hydrolyzed with excess thrombin and hydrolysis products collected by RP-HPLC. The FXIII AP (33−37) V34 NMR sample contained 1.5 mM hydrolyzed peptide and either 0 or 150 μM bovine thrombin in a total volume of 400 μL. The FXIII AP (33−37) V34L NMR sample contained 1.5 mM hydrolyzed peptide and either 0 or 126 μM bovine thrombin. The samples were buffered in 25 mM H_3PO_4, 150 mM NaCl, 0.2 mM EDTA, pH 5.6, and 10% D_2O. All NMR experiments were performed on a Varian Inova 500 MHz spectrometer equipped with a triple resonance probe and pulsed field *z*-axis gradients. Water was suppressed in the 1D and 2D transferred-NOESY experiments with the WET pulse sequence and in the 2D total correlation spectroscopy experiments (TOCSY) with presaturation. Two-dimensional transferred-NOESY experiments of the enzyme−peptide complexes were run at 17 °C with 32 transients, 512 t_1 increments, mixing times of 400 ms, and a spectral width of 5006 Hz. Spectra were processed using FELIX2000 software (Accelrys, San Diego, CA) on a Silicon Graphics O_2 workstation.

RESULTS

Hydrolysis of Substrate-like Peptides by Thrombin. An HPLC assay was employed to monitor rates of hydrolysis of a series of factor XIII activation peptide segments by thrombin. Accumulation of product over time was used in the kinetic fit calculations. The product peptides FXIII AP (28−37), FXIII AP (28−37) V34L, FXIII AP (33−37), and FXIII AP (33−37) V34L all eluted from the Brownlee Aquapore C8 column as distinct peaks from the parent substrates (28−41) and (33−41), and their identities were verified by MALDI-TOF mass spectrometry.

Kinetic Evaluation of Thrombin Hydrolysis of Factor XIII Activation Peptides. Nonlinear regression analysis values for K_m, k_{cat}, and k_{cat}/K_m are shown in Table 2. The experimentally determined RP-HPLC kinetic parameters for the FXIII AP (28−41) V34 peptide are $K_m = 644 \pm 114$ μM, $k_{cat} = 6.2 \pm 0.03$ s^{-1}, and $k_{cat}/K_m = 0.0096 \pm 0.002$ μM^{-1} s^{-1}. The parameters determined for the FXIII AP (28−41) V34L mutant are $K_m = 375 \pm 70$ μM, $k_{cat} = 15.2 \pm 0.02$ s^{-1}, and $k_{cat}/K_m = 0.042 \pm 0.003$ μM^{-1} s^{-1}. The kinetic parameters determined for FXIII AP (33−41) V34 peptide are $K_m = 386 \pm 42$ μM, $k_{cat} = 5.8 \pm 0.02$ s^{-1}, and $k_{cat}/K_m = 0.015 \pm 0.0008$ μM^{-1} s^{-1}. The parameters determined for the FXIII

Table 2: Kinetic Constants for the Hydrolysis of FXIII AP $Arg^{37}-Gly^{38}$ Bonds by Thrombin[a]

substrate peptide	K_m (μM)	k_{cat} (s^{-1})	k_{cat}/K_m ($\mu M^{-1}\,s^{-1}$)
FXIII AP (28−41) WT	644 ± 114	6.2 ± 0.03	0.0096 ± 0.002
FXIII AP (28−41) V34L	375 ± 70	15.2 ± 0.02	0.042 ± 0.003
FXIII AP (33−41) WT	386 ± 42	5.8 ± 0.02	0.015 ± 0.0008
FXIII AP (33−41) V34L	327 ± 44	24.3 ± 0.05	0.074 ± 0.0099

[a] Kinetic constants for the thrombin-catalyzed hydrolysis of peptides based on the FXIII activation peptide segments were determined from an HPLC assay as described in the Experimental Procedures. The results shown here represent the averages of at least three independent experiments. Kinetic values reported were calculated using nonlinear regression analysis methods. The error values correspond to the standard error of the mean (SEM).

AP (33−41) V34L mutant are $K_m = 327 \pm 44$ μM, $k_{cat} = 24.3 \pm 0.05$ s^{-1}, and $k_{cat}/K_m = 0.074 \pm 0.0099$ $\mu M^{-1}\,s^{-1}$.

The kinetic parameters for the FXIII AP (28−41) V34L peptide demonstrate a 1.7-fold improvement in K_m value and a 2.5-fold improvement in k_{cat} value over the FXIII AP (28−41) V34 peptide. Comparing the long and short V34-containing peptides, there is a 1.7-fold decrease in K_m for the FXIII AP (33−41) V34 peptide over the FXIII AP (28−41) V34 peptide, as well as a slight decrease in k_{cat}. Overall, there is a 1.6-fold improvement in k_{cat}/K_m values for the shorter FXIII AP (33−41) peptide relative to FXIII AP (28−41). These kinetic results indicate that truncation of the N-terminal portion of the V34 sequence modestly enhances this peptide's ability to bind to thrombin and does not hinder its cleavage. Kinetic comparisons of the FXIII AP (33−41) V34L and FXIII AP (28−41) V34L results reveal no significant change in K_m for the two mutant peptides. There is, however, a 1.6-fold improvement in k_{cat}, which together with the K_m value leads to a 1.8-fold improvement in the k_{cat}/K_m value for the truncated peptide over the longer sequence. Removal of the N-terminal portion of the V34L-containing peptide allows for more specific interactions with thrombin and faster turnover into product. The wild-type V34 and mutant V34L FXIII AP (33−41) peptides exhibit roughly equivalent K_m values within experimental error. By contrast, the FXIII AP (33−41) V34L peptide shows a 4-fold improvement in k_{cat} over both the truncated wild-type FXIII AP (33−37) and its longer parent peptide. With this improvement in k_{cat}, the FXIII AP (33−41) V34L peptide is the best thrombin substrate of the studied series.

One-Dimensional Line Broadening NMR for Wild-Type and Mutant V34L FXIII Activation Peptide Segments. One-dimensional ^{1}H NMR spectra were acquired for each hydrolyzed FXIII AP-like peptide both free in solution and complexed with thrombin. Line broadening is observed for each of the peptides in complex with thrombin, indicating significant contact with the enzyme surface. A comparison of the spectra for the peptides free in solution and in complex with thrombin reveals no significant changes in chemical shift for peptide protons upon binding to the enzyme.

Figure 1 highlights fingerprint and aliphatic regions of the 1D proton spectra for FXIII AP (33−37) V34. Figure 1A is free peptide and Figure 1B is the peptide−enzyme complex. Line broadening is apparent for residues P_5-P_1, with the most dramatic effects being seen for P_1 residue Arg37 which sits within the active site cleft of thrombin.

Figure 2 illustrates the 1D proton spectra for FXIII AP (33−37) V34L. Greater line broadening is observed for the FXIII AP (33−37) V34L peptide in the presence of thrombin, indicating that this peptide has more extensive contact with the enzyme surface. The resonance of the P_4 residue Leu34 is broadened beyond that of the P_4 residue Val34.

Two-Dimensional Transferred Nuclear Overhauser Effect NMR. The thrombin−peptide complexes likely exhibit fast exchange conditions based on the following observations. The K_m values for hydrolysis of the peptides are in agreement with weak binding. Line broadening is observed at reduced temperatures in the 1D ^{1}H NMR spectra, and large negative NOEs are observed in the transferred-NOESY spectra. There is an increase in the number of NOEs that arise for each peptide in the presence of thrombin. No distorted peaks representing free and bound states are observed for either peptide as reported by Ni et al. (*36*) for the improved thrombin substrate, Fbg Aα (7−16) V15P. The NOEs observed for these truncated FXIII AP-like substrates correspond to through-space interactions between protons which are less than 5 Å apart.

Information about the solution conformation of thrombin-bound FXIII AP segments can be deduced from transferred NOE cross-peaks. Figure 3A exhibits key NOEs observed previously (*27*) for FXIII AP (28−37), and Figure 3B exhibits the corresponding portion of the spectrum for the truncated FXIII AP (33−37). Following the same style of presentation, Figure 4A exhibits key NOEs observed previously (*27*) for FXIII AP (28−37) V34L, and Figure 4B exhibits the corresponding portion of the spectrum for the truncated FXIII AP (33−37) V34L.

In Figures 3B and 4B note that each truncated peptide experiences side-chain to side-chain interactions between V35γ and P36 (δ and/or δ') protons. These nearest-neighbor NOEs were also recorded in the spectra of the longer FXIII AP (28−37) peptides. Both the long and the truncated V34L peptides display an additional NOE between L34δ and P36δ (Figure 4) that does not appear in the spectra of the V34-containing peptides (Figure 3). No through-space interactions are recorded at all between the V34 side chain and the P36 ring protons. Further structural information is obtained from the observation that the two truncated FXIII AP-like peptides contain NOEs between V35α and P36δ/δ' (data not shown). Such through-space interactions are consistent with the presence of a trans conformation about the X−Pro bond of the peptides. The remaining NOEs seen for the peptides were either intraresidue or the anticipated nearest neighbor interresidue interactions. Removal of the N-terminus of FXIII AP (28−37) did not compromise the ability of FXIII activation peptide segments to interact with thrombin.

DISCUSSION

The X-ray crystal structures of thrombin-bound peptides based on Fbg Aα, the FXIII activation peptide, and PAR1 are displayed in Figure 5 along with key residues from the enzyme active site region. The crystal structure of the bound FXIII AP (28−37) V34 depicts the $P_{10}-P_1$ residues (*37*) in a β-turn conformation much like that of the thrombin substrate fibrinogen Aα (7−16) (*35*). Solution NMR data, by contrast, suggest a FXIII AP (28−37) structure in which

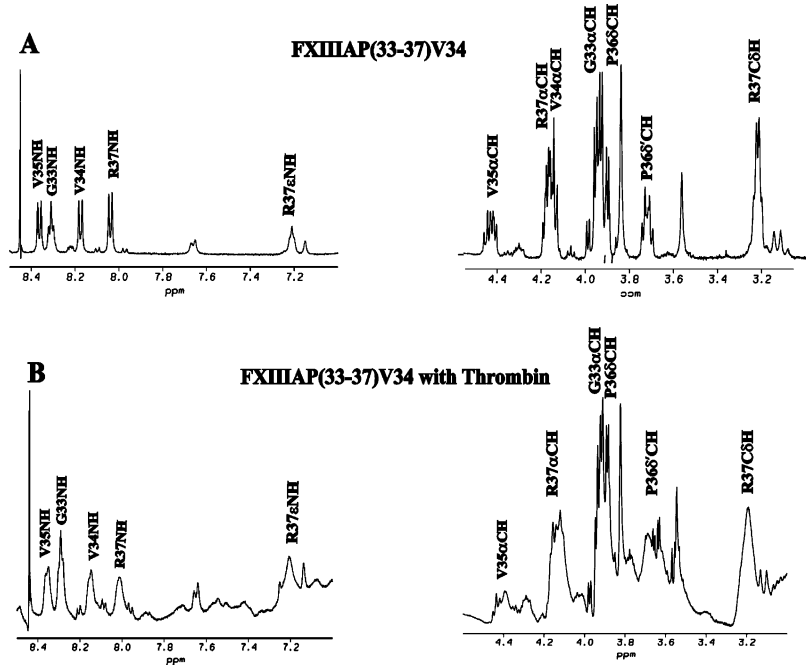

FIGURE 1: Line broadening in 1D proton NMR spectra for factor XIII AP (33−37) V34 in the presence of thrombin. (A) Spectrum for 1.5 mM peptide in solution. (B) Spectrum for 1.5 mM peptide in the presence of 150 μM thrombin. All NMR samples are in 25 mM H_3PO_4, 150 mM NaCl, 200 μM EDTA, and 10% D_2O, pH 5.6 (NMR buffer). The protons that are labeled in the figure make extensive contact with thrombin in the bound state and emphasize the P_4-P_1 positions.

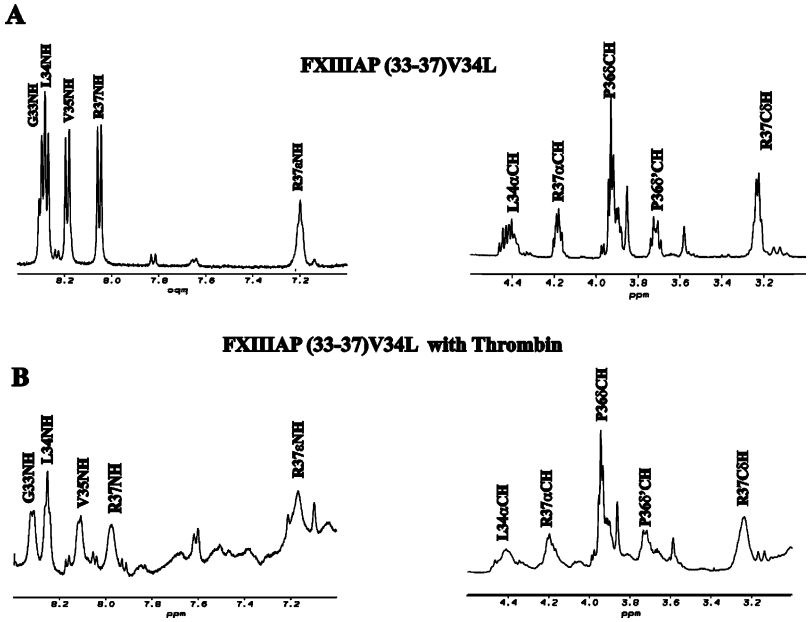

FIGURE 2: Line broadening in 1D proton NMR spectra for factor XIII AP (33−37) V34L in the presence of thrombin. (A) Spectrum for 1.5 mM peptide in solution. (B) Spectrum for 1.5 mM peptide in the presence of 0.126 mM thrombin. The experimental conditions are the same as in Figure 1. More proton line broadening is observed for the mutant V34L peptide than is observed for the wild-type V34 sequence. In agreement with kinetic results, the mutant peptide interacts more effectively with the thrombin surface.

the binding interactions are focused on the P_4-P_1 residues (*27*). This focus is even more apparent with peptides based on the cardioprotective FXIII V34L polymorphism. The conformational features found *in solution* for FXIII activation peptides are thus perhaps more similar to those of a PAR1-like peptide. See Figure 5C. The current study addresses the structural differences between the X-ray and solution NMR data by using truncated versions of FXIII activation peptides. Results reveal that, unlike Fbg Aα (7−16), the FXIII activation peptide N-terminus ($P_{10}-P_6$) is not critical for interaction with thrombin.

Analysis of Kinetic Results. The beneficial effect of the FXIII V34L substitution on thrombin hydrolysis of FXIII AP (28−41) was confirmed in the current study (*15*). The enhancement in K_m and, more importantly, the augmentation in k_{cat} indicate that thrombin binds more readily and cleaves more efficiently an activation peptide with a leucine at the P_4 position. The role that the N-terminal portion of FXIII AP (28−41) plays in promoting the bound conformation and in regulating rates of hydrolysis, however, was not known. The N-terminal segment (28−32) was therefore removed, and peptides based on FXIII AP (33−41) were examined.

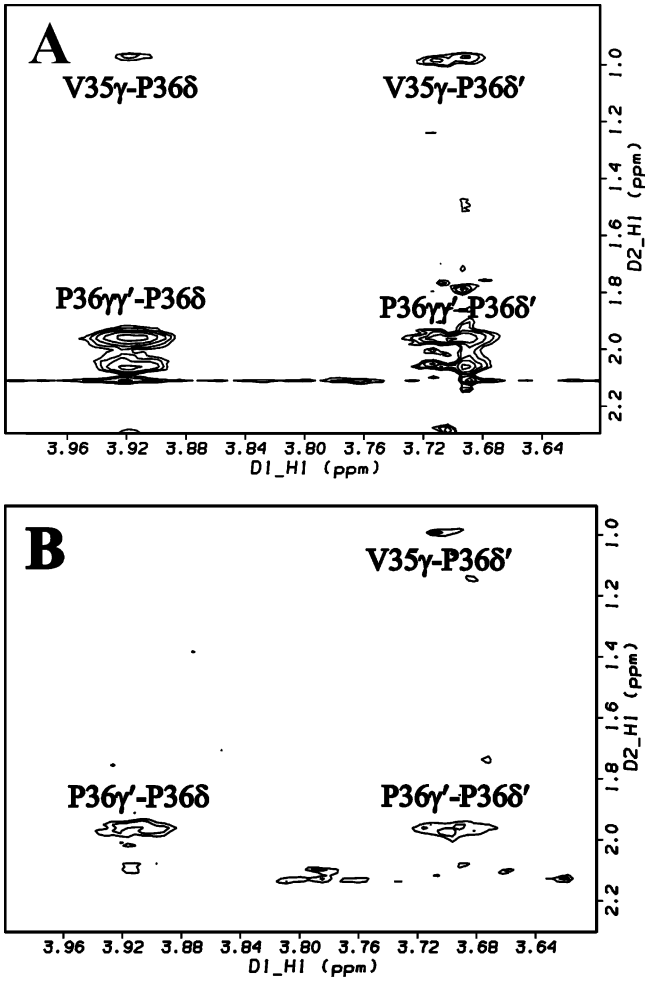

FIGURE 3: Comparison of aliphatic−aliphatic NOEs from 2D transferred-NOESY of V34-containing peptides. (A) 1.5 mM FXIII AP (28−37) V34 in the presence of 0.15 mM thrombin (*27*). (B) 1.5 mM FXIII AP (33−37) V34 in the presence of 0.15 mM thrombin. Both peptides exhibit through-space interactions between the end of the V35 side chain and the P36 *δ* protons. No long-range NOEs are seen with either peptide for V34. Furthermore, in FXIII AP (28−37) V34, no long-range NOEs have been observed involving V29.

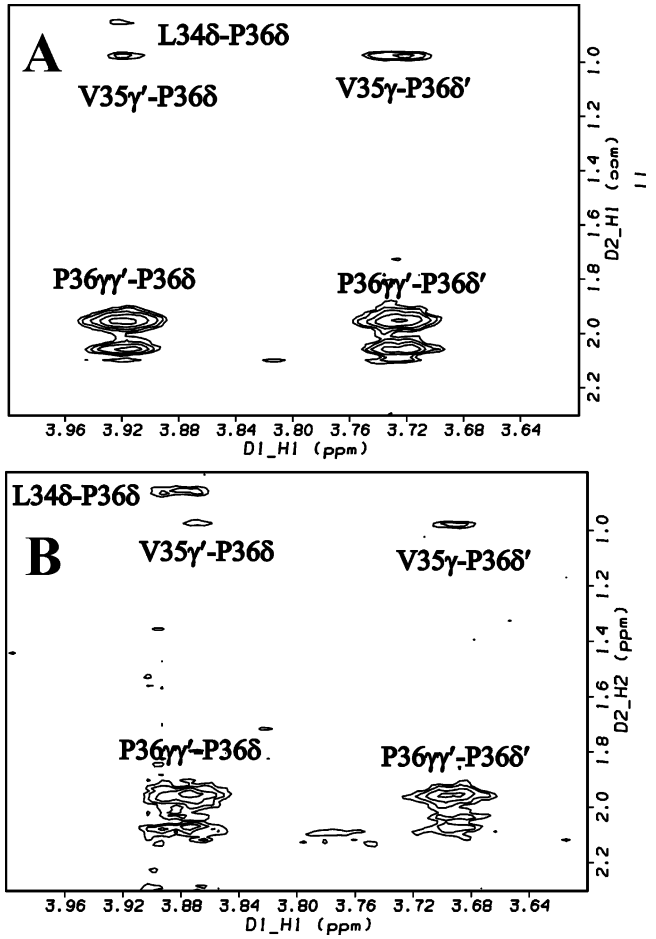

FIGURE 4: Comparison of aliphatic−aliphatic NOEs from 2D transferred-NOESY of V34L containing peptides. (A) 1.5 mM FXIII AP (28−37) V34L in the presence of 0.15 mM thrombin (*27*). (B) 1.5 mM FXIII AP (33−37) V34L in the presence of 0.126 mM thrombin. The critical L36*δ*−P36*δ* interaction is maintained with the truncated peptide. The N-terminal residues 28−32 are not needed to promote this structural feature.

For the wild-type V34 sequence, truncation leads to an improvement in K_m and little change in k_{cat} relative to the longer (28−41) segment. Loss of the N-terminal segment of the activation peptide thus enhances binding to thrombin. FXIII AP (28−41) V34 appears to receive no added benefit from the N-terminus; in fact, it may actually hinder the ability of the peptide to interact with the thrombin surface. By contrast, little change in K_m occurs for the truncated V34L peptide segment versus the longer FXIII AP (28−41) V34L segment, but there is further enhancement of the k_{cat} value. Once again, the N-terminal portion is not a required substrate feature. When comparing the two truncated peptides, FXIII AP (33−41) V34 and FXIII AP (33−41) V34L, it is interesting to note that they exhibit such similar K_m values. The FXIII AP (33−41) V34L peptide, however, remains the superior substrate due to a better than 4-fold improvement in k_{cat} relative to the truncated wild-type sequence. Of the different peptides examined in this study, the truncated FXIII AP (33−41) V34L is the best substrate for thrombin.

The kinetic results obtained with FXIII AP (28−41) and FXIII AP (33−41) are in sharp contrast to what has been observed with Fbg Aα-like segments. For this chain of fibrinogen, the N-terminal P_{10}−P_6 residues are critical for thrombin recognition, binding, and cleavage. Kinetic results on thrombin hydrolysis of fibrinogen and fibrinogen-like peptides (*31*, *43*, *44*) report direct involvement of the Phe at the P_9 position. Marsh et al. (*43*) carried out studies with two peptide segments of the fibrinogen Aα chain: Ac-FLAEGGGVRGP-$NHCH_3$ (defined as the F6 peptide) and Ac-LAEGGGVRGP-$NHCH_3$ (defined as the F7 peptide). The F7 peptide was a poor substrate, and even in the presence of excess thrombin, the kinetic properties of this peptide could not be determined. Attempts to further shorten the peptide and/or extend it in the C-terminal direction also were ineffective. Only when the Phe residue was added to the P_9 position did the Fbg Aα-like peptide become a viable substrate for thrombin (*43*).

More recent studies (*45*) have demonstrated that the Phe at the P_9 position cannot be replaced with the aromatic residue Tyr. Kinetic studies indicate that thrombin has great difficulty in hydrolyzing Fbg Aα F8Y and is completely unable to hydrolyze the peptide Fbg Aα (1−23) F8Y. The X-ray crystal structure (*46*) of this Fbg Aα-like peptide in complex with thrombin reveals a large shift in the carbonyl oxygen of Tyr8 relative to Phe8 that distorts the geometry

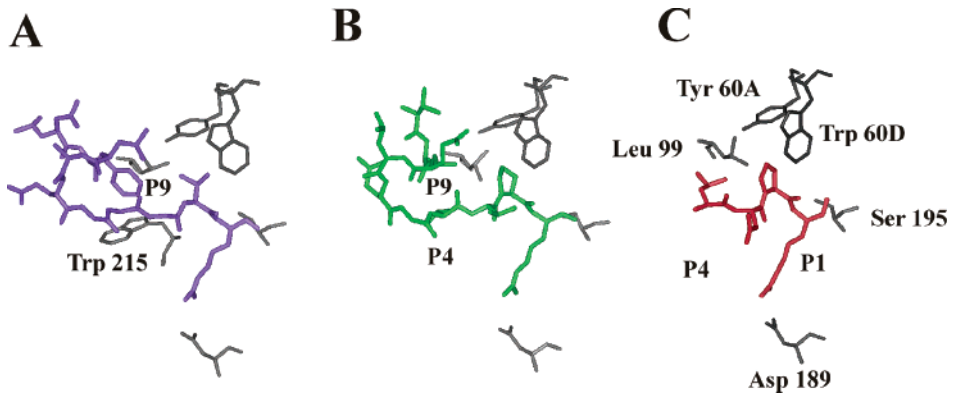

FIGURE 5: Comparison of the X-ray crystal structures of three substrate-like peptides bound to the active site region of thrombin: (A) fibrinogen Aα (7−16) in blue, PDB 1BBR (*35*); (B) FXIII AP (28−37) in green, PDB 1FIE (*37*); and (C) PAR1 (38−41) in red, PDB 1NRS (*29*). Selected thrombin residues are displayed in black. Fibrinogen Aα is highly dependent on the Phe8 at the P_9 position. PAR1 focuses on the P_4 through P_1 positions to bind effectively to thrombin. The X-ray crystal structure of bound FXIII AP (28−37) exhibits features similar to both of these substrates.

of the peptide at the catalytic site, resulting in a poor substrate for thrombin. By contrast, the wild-type segment of Fbg Aα (7−16) utilizes the Phe8 at the P_9 position as part of a hydrophobic cluster that optimizes interactions with the thrombin active site surface (*31*−*36*, *43*). This Phe participates in beneficial $\pi-\pi$ stacking interactions with thrombin Trp215. See Figure 5A for the X-ray crystal structure of this thrombin-bound peptide (*35*).

Our own efforts to create a FXIII AP analogue to Fbg Aα (7−20) in which the P_9 Val was mutated to Phe did result in an improved thrombin substrate relative to FXIII AP (28−41) V34 (*27*). However, the peptide did not exhibit kinetics as effective as Fbg Aα (7−20). It is likely that the FXIII AP (28−41) V29F sequence experiences some steric issues that Fbg Aα (7−20) can overcome with its three Gly residues (^{12}GGG^{14}). These small amino acids at positions P_5-P_3 could promote the greater flexibility needed to make a β-turn, an important structural feature of Fbg Aα (7−20). The residues N-terminal to the Arg37−Gly38 bond of the FXIII activation peptide (^{33}GVV^{35}) are bulkier than the three Gly residues and do not allow the peptide as much elasticity to firmly place the Phe at the P_9 residue in an optimal position to increase thrombin hydrolysis.

The kinetic results presented here indicate that removal of the FXIII AP N-terminus has no adverse effects on thrombin's ability to bind and hydrolyze the shortened peptides. The truncations actually have beneficial effects. The wild-type FXIII AP (33−41) V34 sequence exhibits a decrease in K_m relative to the longer (28−41) sequence whereas the mutant FXIII AP (33−41) V34L sequence exhibits a further increase in k_{cat} relative to its longer sequence. Solution NMR studies reveal the structural features that these truncated peptides maintain to continue as effective substrates for thrombin.

Examining Structural Features Assumed by FXIII AP (33−*37) When in Complex with Thrombin.* The FXIII AP (28−37) peptides encompass the $P_{10}-P_1$ residues whereas the FXIII AP (33−37) peptides include only the P_5-P_1 residues. Both the V34 and the L34 truncated peptides exhibit significant line broadening, indicating considerable contact with the enzyme surface. With these truncated peptides, more extensive aliphatic proton line broadening continues to be observed for the L34-containing peptide relative to that of V34. This increased broadening provides a structural basis for the improved kinetics of the L34 peptides (see Figures 1 and 2). As seen in other FXIII AP segments, the V35 side chain at position P_3 makes less contact with the enzyme surface as line broadening is not as extensive for this amino acid residue (data not shown and refs *27*, *47*, and *48*). X-ray crystallographic studies indicate that the P_3 amino acid residue of thrombin substrates is often directed away from the active site (*29*).

Transferred-NOESY spectra of the truncated peptides provide valuable information about the bound conformation of these peptides. Previously reported 2D transferred-NOESY studies with the FXIII AP (28−41) V34 and V34L peptides indicated no long-range NOEs were visible from the N-terminal $P_{10}-P_8$ residues toward the P_4-P_1 residues (*27*). Such results suggest that the N-terminal segment is positioned greater than 5 Å from the C-terminal P_4-P_1 residues. If the N-terminal segment plays a critical role in defining the bound conformation, a deletion would likely have a major effect on the structural features of the truncated activation peptides in the presence of thrombin. The residues anticipated to be most affected by such a change would be the P_4-P_1 residues. This sort of structural disruption, however, is not observed.

Characteristic NOEs involving V35γ−P36 (δ and/or δ') (Figures 3 and 4) and V35α−P36δ (data not shown) continue to be seen in the truncated peptides. As with the longer FXIII AP (28−37) series, the V35 α and γ protons of the truncated peptides are oriented in proximity to the P36δ ring proton. Furthermore, the V35−P36 peptide bond is in the trans conformation. For both of the V34-containing peptides, FXIII AP (33−37) and FXIII AP (28−41), no NOEs are visible from the V34 to the P36. It is likely that the side chain of V34 is too short to influence the relaxation properties of P36. By contrast, L34 with its extra methylene group is able to generate NOEs between L34δ and P36δ (Figure 4). This characteristic NOE is maintained in both the long and the truncated FXIII AP L34 segments. There are no visible NOEs between the R37 side chain and P36 for all of the peptides, indicating the arginine side chain is positioned firmly within the active site cleft of thrombin. The remaining intra- and interresidue NOEs observed for both truncated peptides are quite comparable. As a result, the solution conformations of the thrombin-bound FXIII AP (33−37) V34 and L34

peptides are expected to be very similar. The extra L34−P36 interactions should promote more effective contact with the apolar binding region of the thrombin active site.

Correlating the Kinetic and Structural Results for the FXIII AP (33−37) Segments with Other Thrombin Substrates. Sadasivan and Yee published X-ray crystal structures of the peptide FXIII AP (28−37) bound to thrombin (*37*). Two different complexes were observed within the unit cell including PEP1 bound to the thrombin MOL1 and PEP2 bound to MOL2. PEP1 depicts the FXIII AP (28−37) interacting with thrombin in a manner very similar to that of Fbg Aα (7−16). See Figure 5A,B. Both X-ray and solution NMR studies have described the bound structure of the Aα peptide as having a β-turn conformation that promotes formation of a hydrophobic cluster involving Fbg Aα F8, L9, G13, and V15 (*32*−*36*). The PEP1 structure for FXIII AP (28−37) V34 exhibits a similar β-turn conformation with interproton distances from the V29 side chain to V35 and P36 that should give rise to NOEs. These long-range distances, however, are not seen in the solution NMR studies reported by Trumbo and Maurer (*27*) for FXIII AP (28−37) V34 segments. The X-ray crystal structure of PEP2 (*37*) displays the same type of turn, but the interproton distances from V29 to residues V35 and P36 are less likely to give rise to NOEs.

The structural differences between PEP1 and PEP2 can be mapped to differences in interaction of the FXIII activation peptide with the thrombin molecules MOL1 and MOL2. Both PEP2 and MOL2 have significantly larger *B* values, correlated with a greater degree of disorder, than PEP1 and MOL1 (*37*). The N-terminal portion of PEP2 is most affected. On the basis of 2D transferred-NOESY data and the X-ray crystal results, we have proposed (*27*) that if a β-turn conformation exists for the wild-type FXIII AP segment, the protons involved are either too distant from one another to give rise to NOEs or the tighter conformation is fleeting in nature.

Sadasivan and Yee also present preliminary structural data on FXIII AP (28−37) V34L bound to thrombin. X-ray crystal and modeling studies indicate that the L34 substitution leads to a different peptide conformation (coordinates not released) (*37*). These results suggest that the β-turn conformation is not preserved in the mutant. A review of PEP1 bound to thrombin indicates that FXIII V34 enters into the thrombin aryl binding site, a key region occupied by Fbg Aα F8. Binding of FXIII V34 at this site leads to changes in the side-chain positions of thrombin I174 and W215. A L34 side chain would cause further disruptions, making it difficult to maintain the same β-turn conformation (*37*). Our solution NMR studies with both long and truncated FXIII AP segments (V34 and L34) all support the lack of a tight β-turn conformation. Such results thus correlate with the FXIII AP (28−37) L34 X-ray data. Structural emphasis is placed on maintaining key P_4 through P_1 contacts within the thrombin surface.

The P_4−P_1 residues of FXIII AP V34L (^{34}LVPR^{37}) exhibit features resembling those of PAR1 (^{38}LDPR^{41}). Of particular importance are the Leu at P_4 and the Pro at P_2 (*29*). One-dimensional proton line broadening NMR studies (*28*) reveal that the N-terminal portion of the PAR1 (32−41) peptide makes little contact with the thrombin active site surface as was observed for FXIII AP (28−37). Furthermore, both 2D transferred-NOESY (*28*) and X-ray crystal studies (*29*) indicate that the critical P_4 to P_2 interactions between Leu and Pro exist for the PAR1 peptide in the presence of thrombin. The PAR1 L38 is positioned within the apolar binding site, and its side chain is directed toward thrombin L99. See Figure 5C. The PAR1 L38 is oriented to interact with PAR1 P40 that is situated beneath the thrombin Trp 60D insertion loop.

On the basis of our kinetic and NMR results, we continue to propose that the FXIII AP segments assume conformations more similar to those of PAR1 than fibrinogen Aα. The need for a β-turn conformation is very likely unique to fibrinogen Aα due to its nonoptimal P_4−P_1 residues. Fbg Aα F8 plays a key role in establishing a productive conformation and benefits greatly from thrombin W215 in the aryl binding site. Di Cera and co-workers have demonstrated that when this tryptophan is converted to an alanine (W215A), thrombin's ability to hydrolyze fibrinogen Aα is severely compromised (*49*, *50*). PAR1, which does not rely so heavily on the aryl binding site, remains a viable thrombin substrate. In solution, the side chain of FXIII L34, and perhaps also V34, is predicted to be oriented more toward the apolar binding site than to the aryl binding site. Such an arrangement would promote the beneficial L34 to P36 interactions.

Sadasivan and Yee were clearly able to capture wild-type FXIII AP (28−37) V34 in a β-turn conformation similar to that adopted by Fbg Aα (7−16). Results from solution studies, however, suggest that the N-terminal P_{10}−P_6 residues of FXIII AP (28−37) are not necessary for substrate recognition by thrombin. By contrast, fibrinogen Aα (7−16) must adopt a turn conformation that is highly dependent upon Phe8 at the P_9 position to serve as a viable substrate to thrombin. It is possible that wild-type FXIII AP (1−37), containing a much longer N-terminal segment, has a greater propensity to assume the β-turn character. We propose that this conformational feature is less likely to be a governing element than the P_4−P_1 residues. Kinetic and solution NMR studies suggest that FXIII activation peptides bind to thrombin in a manner more like PAR1 rather than fibrinogen Aα.

ACKNOWLEDGMENT

We thank A. F. Spatola and F. M. Brunel for training in peptide synthesis, T. A. Trumbo for guidance in thrombin purification and enzyme kinetics, and N. J. Stolowich for assistance in NMR methods. Furthermore, we appreciate helpful discussions with T. A. Trumbo, B. T. Turner, T. M. Sabo, and D. B. Cleary during the course of this project.

REFERENCES

1. Stubbs, M. T., and Bode, W. (1993) A player of many parts: the spotlight falls on thrombin's structure, *Thromb. Res. 69*, 1−58.
2. Mann, K. G. (2003) Thrombin Formation, *Chest 124* (3 Suppl.), 4S−10S.
3. Di Cera, E. (2003) Thrombin Formation, *Chest 124* (3 Suppl.), 11S−17S.
4. Mosesson, M. W., Siebenlist, K. R., and Meh, D. A. (2001) The structure and biological features of fibrinogen and fibrin, *Ann. N.Y. Acad. Sci. 936*, 11−30.
5. Lorand, L. (2001) Factor XIII: Structure, activation, and interactions with fibrinogen and fibrin, *Ann. N.Y. Acad. Sci. 936*, 291−311.

6. Naski, M. C., Lorand, L., and Shafer, J. A. (1991) Characterization of the kinetic pathway for fibrin promotion of alpha-thrombin-catalyzed activation of plasma factor XIII, *Biochemistry 30*, 934−941.
7. Lewis, S. D., Janus, T. J., Lorand, L., and Shafer, J. A. (1985) Regulation of formation of factor XIIIa by its fibrin substrates, *Biochemistry 24*, 6772−6777.
8. Hornyak, T. J., and Shafer, J. A. (1992) Interactions of factor XIII with fibrin as substrate and cofactor, *Biochemistry 31*, 423−429.
9. Philippou, H., Rance, J., Myles, T., Hall, S. W., Ariens, R. A., Grant, P. J., Leung, L., and Lane, D. A. (2003) Roles of low specificity and cofactor interaction sites on thrombin during factor XIII activation, *J. Biol. Chem. 278*, 32020−32026.
10. Kohler, H. P., and Grant, P. J. (1999) The role of factor XIIIVal34Leu in cardiovascular disease, *Q. J. Med. 92*, 67−72.
11. McCormack, L. J., Kain, K., Catto, A. J., Stickland, M. H., and Grant, P. J. (1998) Prevalence of FXIII V34L in populations with different cardiovascular risk, *Thromb. Haemostasis 80*, 523−524.
12. Ariens, R. A., Philippou, H., Nagaswami, C., Weisel, J. W., Lane, D. A., and Grant, P. J. (2000) The factor XIII V34L polymorphism accelerates thrombin activation of factor XIII and affects cross-linked fibrin structure, *Blood 96*, 988−995.
13. Ariens, R. A., Lai, T. S., Weisel, J. W., Greenberg, C. S., and Grant, P. J. (2002) Role of factor XIII in fibrin clot formation and effects of genetic polymorphisms, *Blood 100*, 743−754.
14. Lim, B. C., Ariens, R. A., Carter, A. M., Weisel, J. W., and Grant, P. J. (2003) Genetic regulation of fibrin structure and function: complex gene-environment interactions may modulate vascular risk, *Lancet 361*, 1424−1431.
15. Trumbo, T. A., and Maurer, M. C. (2000) Examining thrombin hydrolysis of the factor XIII activation peptide segment leads to a proposal for explaining the cardioprotective effects observed with the factor XIII V34L mutation, *J. Biol. Chem. 275*, 20627−20631.
16. Coughlin, S. R. (2000) Thrombin signaling and protease-activated receptors, *Nature 407*, 258−264.
17. O'Brien, P. J., Molino, M., Kahn, M., and Brass, L. F. (2001) Protease activated receptors: theme and variations, *Oncogene 20*, 1570−1581.
18. Vu, T. K., Wheaton, V. I., Hung, D. T., Charo, I., and Coughlin, S. R. (1991) Domains specifying thrombin-receptor interaction, *Nature 353*, 674−677.
19. Kahn, M. L., Zheng, Y. W., Huang, W., Bigornia, V., Zeng, D., Moff, S., Farese, R. V., Jr., Tam C., and Coughlin, S. R. (1998) A dual thrombin receptor system for platelet activation, *Nature 394*, 690−694.
20. Xu, W. F., Andersen, H., Whitmore, T. E., Presnell, S. R., Yee, D. P., Ching, A., Gilbert, T., Davie, E. W., and Foster, D. C. (1998) Cloning and characterization of human protease-activated receptor 4, *Proc. Natl. Acad. Sci. U.S.A. 95*, 6642−6646.
21. Vindigni, A., Dang, Q. D., and Di Cera, E. (1997) Site-specific dissection of substrate recognition by thrombin, *Nat. Biotechnol. 15*, 891−895.
22. Le Bonniec, B. F., Myles, T., Johnson, T., Knight, C. G., Tapparelli, C., and Stone, S. R. (1996) Characterization of the P2′ and P3′ specificities of thrombin using fluorescence-quenched substrates and mapping of the subsites by mutagenesis, *Biochemistry 35*, 7114−7122.
23. Backes, B. J., Harris, J. L., Leonetti, F., Craik, C. S., and Ellman, J. A. (2000) Synthesis of positional-scanning libraries of fluorogenic peptide substrates to define the extended substrate specificity of plasmin and thrombin, *Nat. Biotechnol. 18*, 187−193.
24. Ichinose, A., and Davie, E. W. (1988) Characterization of the gene for the a subunit of human factor XIII (plasma transglutaminase), a blood coagulation factor, *Proc. Natl. Acad. Sci. U.S.A. 85*, 5829−5833.
25. Watt, K. W., Cottrell, B. A., Strong, D. D., and Doolittle, R. F. (1979) Amino acid sequence studies on the alpha chain of human fibrinogen. Overlapping sequences providing the complete sequence, *Biochemistry 18*, 5410−5416.
26. Vu, T. K., Hung, D. T., Wheaton, V. I., and Coughlin, S. R. (1991) Molecular cloning of a functional thrombin receptor reveals a novel proteolytic mechanism of receptor activation, *Cell 64*, 1057−1068.
27. Trumbo, T. A., and Maurer, M. C. (2002) Thrombin hydrolysis of V29F and V34L mutants of factor XIII (28−41) reveals roles of the P_9 and P_4 positions in factor XIII activation, *Biochemistry 41*, 2859−2868.
28. Ni, F., Ripoll, D. R., Martin, P. D., and Edwards, B. F. (1992) Solution structure of a platelet receptor peptide bound to bovine alpha-thrombin, *Biochemistry 31*, 11551−11557.
29. Mathews, I. I., Padmanabhan, K. P., Ganesh, V., Tulinsky, A., Ishii, M., Chen, J., Turck, C. W., Coughlin, S. R., and Fenton, J. W., II (1994) Crystallographic structures of thrombin complexed with thrombin receptor peptides: existence of expected and novel binding modes, *Biochemistry 33*, 3266−3279.
30. Ishii, K., Gerszten, R., Zheng, Y. W., Turck, C. W., and Coughlin, S. R. (1995) Determinants of thrombin receptor cleavage. Receptor domains involved, specificity, and role of the P_3 aspartate, *J. Biol. Chem. 270*, 16435−16440.
31. Van Nispen, J. W., Hageman, T. C., and Scheraga, H. A. (1977) Mechanism of action of thrombin on fibrinogen. The reaction of thrombin with fibrinogen-like peptides containing 11, 14, and 16 residues, *Arch. Biochem. Biophys. 182*, 227−243.
32. Ni, F., Konishi, Y., Frazier, R. B., Scheraga, H. A., and Lord, S. T. (1989) High-resolution NMR studies of fibrinogen-like peptides in solution: interaction of thrombin with residues 1−23 of the fibrinogen Aα chain of human fibrinogen, *Biochemistry 28*, 3082−3094
33. Ni, F., Meinwald, Y. C., Vasquez, M., and Scheraga, H. A. (1989) High-resolution NMR studies of fibrinogen-like peptides in solution: structure of a thrombin-bound peptide corresponding to residues 7−16 of the Aα chain of human fibrinogen, *Biochemistry 28*, 3094−3105.
34. Stubbs, M. T., Oschkinat, H., Mayr, I., Huber, R., Angliker, H., Stone, S. R., Bode, W. (1992) The interaction of thrombin with fibrinogen. A structural basis for its specificity, *Eur. J. Biochem. 1*, 187−195.
35. Martin, P. D., Robertson, W., Turk, D., Huber, R., Bode, W., and Edwards, B. F. (1992) The structure of residues 7−16 of the A alpha-chain of human fibrinogen bound to bovine thrombin at 2.3-Å resolution, *J. Biol. Chem. 267*, 7911−7920.
36. Ni, F., Zhu, Y., and Scheraga, H. A. (1995) Thrombin-bound structures of designed analogs of human fibrinopeptide A determined by quantitative transferred NOE spectroscopy: a new structural basis for thrombin specificity, *J. Mol. Biol. 252*, 656−671.
37. Sadasivan, C., and Yee, V. C. (2000) Interaction of the factor XIII activation peptide with alpha-thrombin. Crystal structure of its enzyme−substrate analog complex, *J. Biol. Chem. 275*, 36942−36948.
38. Winzor, D. J., and Scheraga, H. A. (1964) Titration Behavior of Bovine Thrombin, *Arch. Biochem. Biophys. 104*, 202−207.
39. Bode, W., Turk, D., and Karshikov, A. (1992) The refined 1.9-Å X-ray crystal structure of D-Phe-Pro-Arg chloromethyl ketone-inhibited human alpha-thrombin: structure analysis, overall structure, electrostatic properties, detailed active-site geometry, and structure−function relationships, *Protein Sci. 1*, 426−471.
40. Dang, Q. D., Sabetta, M., and Di Cera, E. (1997) Selective loss of fibrinogen clotting in a loop-less thrombin, *J. Biol. Chem. 272*, 19649−19651.
41. Campbell, A. P., and Sykes, B. D. (1993) The two-dimensional transferred nuclear Overhauser effect: theory and practice, *Annu. Rev. Biophys. Biomol. Struct. 22*, 99−122.
42. Ni, F. (1994) Recent Developments in Transferred NOE Methods, *Prog. NMR Spectrosc. 26*, 517−606.
43. Marsh, H. C., Jr., Meinwald, Y. C., Lee, S., and Scheraga, H. A. (1982) Mechanism of action of thrombin on fibrinogen. Direct evidence for the involvement of phenylalanine at position P_9, *Biochemistry 21*, 6167−6171.
44. Scheraga, H. A. (1983) Interaction of thrombin and fibrinogen and the polymerization of fibrin monomer, *Ann. N.Y. Acad. Sci. 408*, 330−343.
45. Rooney, M. M., Mullin, J. L., and Lord, S. T. (1998) Substitution of tyrosine for phenylalanine in fibrinopeptide A results in preferential thrombin cleavage of fibrinopeptide B from fibrinogen, *Biochemistry 37*, 13704−13709.
46. Malkowski, M. G., Martin, P. D., Lord, S. T., and Edwards, B. F. (1997) Crystal Structure of fibrinogen Aα peptide 1−23 (F8Y) bound to bovine thrombin explains why the mutation of Phe-8 to tyrosine strongly inhibits normal cleavage at Arg-16, *Biochem. J. 326*, 815−822.
47. Trumbo, T. A., and Maurer, M. C. (2003) V34I and V34A substitutions within the factor XIII activation peptide segment (28−41) affect interactions with the thrombin active site, *Thromb. Haemostasis 4*, 647−653.

48. Isetti, G., and Maurer, M. C. (2004) Probing thrombin's ability to accommodate a V34F substitution within the factor XIII activation peptide segment (28−41), *J. Pept. Res.* (in press).
49. Arosio, D., Youhna, A. M., and Di Cera, E. (2000) Mutation of W215 compromises thrombin cleavage of fibrinogen but not of PAR-1 or protein C, *Biochemistry 39*, 8095−8101.
50. Ayala, A. M., Arosio, D., and Di Cera, E. (2001) Mutation of W215 compromises thrombin cleavage of fibrinogen, but not PAR1 or protein C, *Ann. N.Y. Acad. Sci. 936*, 456−458.

BI049796V